ISSN 0102-745X

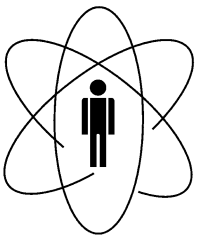

CBPF - CENTRO BRASILEIRO DE PESQUISAS FÍSICAS

Rio de Janeiro

Notas Técnicas

CBPF-NT-002/18

fevereiro 2018

Porous medium permeability estimation for well imagery and characterization using complex resistivity spectra

Manuel Blanco Valentín, Márcio P. de Albuquerque, Marcelo P. de Albuquerque, Elisângela L. Faria, Yann Le Guével, Clécio Roque de Bom and Maury D. Correia

MINISTÉRIO DA CIÊNCIA, TECNOLOGIA, INOVAÇÕES E COMUNICAÇÕES

dx.doi.org/10.7437/NT2236-7640/2018.01.002
Notas Técnicas,v. 8, n. 1, p. 17–24, 2018

Porous medium permeability estimation for well imagery and characterization using complex resistivity spectra

Manuel Blanco Valentín,* Márcio P. de Albuquerque,† Marcelo P. de Albuquerque,‡ e Elisângela L. Faria§
Coordenação de Atividades Técnicas (CAT/CBPF),
Centro Brasileiro de Pesquisas Físicas
Rua Dr. Xavier Sigaud, 150, Ed. César Lattes,
Urca, Rio de Janeiro, RJ. CEP 22290-180, Brasil

Yann Le Guével¶
Telecom Physique Strasbourg,
Pole API, 300 Bd Sébastien Brant,
67400 Illkirch-Graffenstaden, France

Clécio Roque de Bom**
Centro Federal de Educação Tecnológica Celso Suckow da Fonseca,
Rodovia Mário Covas, lote J2, quadra J
Distrito Industrial de Itaguaí,
Itaguaí - RJ. CEP: 23810-000, Brasil

Maury D. Correia††
Centro de Pesquisas e Desenvolvimento Leopoldo Américo Miguez de Mello – CENPES
PETROBRAS, Av. Horácio Macedo,
950, Cidade Universitária,
Rio de Janeiro, RJ. CEP 21941-915, Brasil
Submetido: 13/09/2017 *Aceito: 22/02/2018*

Abstract: Formation permeability plays a crucial role in oil/gas industry as it helps geologists understand how the soil was formed and the most likely location of a certain reservoir. It also aids engineers and analysts to know whether that reservoir is exploitable or not. However, these measurements are very costly and difficult to obtain. In the past decades, several methods have appeared for estimating permeability from different sources like Nuclear Magnetic Resonance data or well-logs. In this work we tested the relationship between complex impedance spectra and permeability measurements, showing that –for the tested porous medium– it does exist a correlation of almost 98% between the obtained complex electrical impedance spectra and the permeability of those mediums. This link could be used in the oil/gas industry adapting the current electrical imaging tools to perform sweep measurements instead of single-frequency measurements, which could be used, in theory, to obtain permeability measurements with spacial resolution. On the other hand, we also designed and implemented an imaging tool that relies on this principle to obtain complex impedance volume images.

Keywords: Complex Resistivity Spectra, Permeability Estimation, Porosity, Borehole Image, Oil, Reservoir.

Resumo: As medidas de permeabilidade de formação são chave no relacionado à caracterização de solos. Este parámetro tem um papel fundamental na indústria de gás e óleo, pois ajuda os geólogos a entender como um certo solo foi formado e a possível e mais provável localização de um certo reservatório; e ajuda os engenheiros e analistas a saber se um certo reservatório é explorável ou não. No entanto, medidas de permeabilidade são muito custosas e difíceis de se obter. Nas últimas décadas apareceram novos métodos de estimativa da permeabilidade a partir de fontes de dados como Resonância Magnética Nuclear ou logs de poços. Neste trabalho testamos a relação que medidas de impedância complexa têm com medidas de permeabilidade, provando que –para os médios porosos testados– existe uma correlação de quase 98% entre os espectros de impedância complexa obtidos e a permeabilidade desses médios. Esta relação poderia ser utilizada na indústria de óleo e gás adaptando os sistemas de imageamento elétricos atuais para realizar varreduras de frequência, ao invés de medidas monofrequenciais, as quais poderiam ser posteriormente usadas para criar imagens de permeabilidade estimada. Por outro lado, também realizamos o design e implementação de uma ferramenta de imageamento baseada no princípio de obtenção de imagens de espectros complexos impedância elétrica.

Palavras chave: Espectro de resistividade complexa, estimativa de permeabilidade, porosidade, imagem borehole, óleo, reservatório.

*Electronic address: mbvalentin@cbpf.br

†Electronic address: mpa@cbpf.br

1. INTRODUCTION

When it comes to extracting fossil fuels from the soil, finding them may not be the most important task to achieve. In reality, one must characterize the reservoir first in order to be as sure as possible that it will be feasible to extract the resources contained there. That is the reason why before starting any kind of reservoir exploitation or before drilling any well, there must be a huge effort to try to understand all the petrophysical properties of that specific field soil. This process is usually called *Reservoir/Field Characterization*, which is a multidisciplinary field involving areas of knowledge such as Physics, Statistical Mathematics, Mechanical and Electronics Engineering, Computer Sciences and, of course, Geology.

Reservoir characterization requires the gathering of as much information as possible. There are several possible measurements that could be obtained from the soil, however the most common (see [1]) are seismic 3D measurements and well-logging measurements.

A common workflow is to first sweep a large area (several square kilometers) using a seismic tool, which results on a huge volume of data that allows geologists to induce the possible presence of a reservoir (see [2]). Once the most likely spots to contain oil are located in the field, drilling tasks begin and several wells are opened. The main goal of these tasks are not yet to extract oil, but rather to introduce several logging tools to get even more information about the characteristics of that field. This process is called *Well Logging*. Differently from the seismic data, Well-Log data is very heterogeneous as it is based on several tools, each one of which measures a unique physical property (see [3]).

At the end, these measures offer to geologists information regarding the type of rock that composes the soil, the density of those mediums, their porosity and their electrical or acoustic impedance, to name a few. Even with such much information about the field, this process lacks one of the most important measurements for reservoir characterization: formation permeability. The permeability of the soil is very important because it helps geologists understand how that soil was formed over the years and it is directly related to how easily the exploitation of that reservoir will be. Even so, obtaining permeability measurements from the soil usually requires physical tests that can only be made on the laboratory, In order to do so, it is required to extract core plugs[1] from the drilled well and send them to dedicated facilities. Obtaining these plugs for a significant amount of data in a field makes this process very expensive, although necessary.

Nevertheless, since G. E. Archie proved in 1942 (see [4]) the existence of a correlation between electrical measurements of a fluid contained inside a porous medium and some of its petrophysical properties –such as porosity and permeability– there has been a major effort on exploiting this relation. Electrical measurements are much easier to obtain than permeability laboratory tests and their resolution has evolved very much over the past decades. Nowadays, electrical borehole images are usually used for plane fractures location and characterization (see [5]).

This work is twofold. First, following the task of several authors that have exploited the relationship G. E. Archie first established, and we present a relationship between the permeability of some free porous mediums and their complex resistivity spectra, proving that that same relationship is not only valid for single plug measurements, but also for wireline measurements.

Secondly, we apply this concept by building a resistivity imaging tool that allows us to obtain a complex electrical impedance image of porous mediums. This proof represents a new possibility for well-logging that might allow engineers to create estimated permeability images from electrical borehole images by using the relation between these complex impedance spectra and permeability measures as we explore in this paper, which would be very helpful for reservoir characterization purposes.

This paper is organized as follows: In Section 2 we introduce the theory behind the relation between petrophysical properties and electrical properties, as well as the concept of complex resistivity spectra and its link to those properties. In Section 3 we present the fluids and mediums that we have used in our tests for characterization and imaging purposes. In Section 4 we explain the methodology used for obtaining complex resistivity spectra for single-curve and imaging tests; as well as we introduced the complex resistivity imaging system we designed and implemented for this paper. In Section 5 we present the results of our tests and in Section 6 we discuss these results and explain our interpretation of them.

2. FLUID PERMEABILITY AND WELL CHARACTERIZATION

As introduced before, permeability is one of the key measurements that help geologists figure out the internal structure and properties of a certain soil. This property can be defined as the ability that a porous medium has to allow a certain fluid to flow through it, and it can be calculated using a derivation of Darcy's law (see [6]), as shown in (1),

$$v = \frac{\kappa}{\mu}\left(\frac{\partial p}{\partial x}\right) \tag{1}$$

where v is the superficial fluid flow velocity through the medium, μ is the dynamic viscosity of the fluid, the coefficient $\frac{\partial p}{\partial x}$ represents the variation of the applied pressure over the thickness of the porous medium bed and κ is the medium permeability. Permeability κ is usually expressed in milidarcies (mD) and it can range from values smaller than one to

‡Electronic address: marcelo@cbpf.br
§Electronic address: elisangela@cbpf.br
¶Electronic address: yann.le˙guevel@etu.unistra.fr
**Electronic address: debom@cbpf.br
††Electronic address: maury.duarte@petrobras.com.br

[1] Core Plugs: small cylinders of rock extracted from the well core and used for laboratory analysis to obtain information of the drilled soil such as permeability.

values higher than 50,000 mD. High values of permeability represent mediums that allow the flow of fluid through them easily, while low values of permeability usually indicate the presence of a much hard, highly-compacted medium.

Looking at (1) we can understand why obtaining permeability measurements is a difficult task: it requires the application of a flow-stream, under very controlled conditions (pressure, thickness of the medium bed and flow state) in order to obtain reliable measures. The American Petroleum Institute recommends, on their recommended practices for core analysis (see [7]), the best way of doing such tests on core plugs –for some considerations about permeability measurements on special conditions and with special fluids see [8]–. Creating a well-logging tool that could obtain direct measures of permeability from the well wall has proved to be an almost impossible achievement.

For those reasons the estimation of permeability using other properties–which can be traced back to 1968, see [9]– has become a very important field in the past decades. Several authors have been able to estimate permeability measurements using computational methods and well-logs such as Gamma Ray (GR), Neutron Porosity (NPHI) or Bulk Density (RHOB) (see [10–13]), while others have used NMR[2] logs for that same purpose (see [14, 15]).

2.1. Relation between electrical impedance and porosity

In 1942 G. E. Archie introduced an equation that related the electrical impedance of a certain fluid saturated rock to its porosity (see [4]). This equation is shown in (2),

$$R_t = a \cdot \phi^{-m} \cdot S_w^{-n} \cdot R_w \tag{2}$$

where R_t is the resistivity of the fluid saturated rock, R_w is brine resistivity, S_w is the fluid brine saturation, a is the tortuosity factor of the medium, m and n are cementation and saturation exponent –respectively– and ϕ is the porosity of the medium.

This relationship was a very important breakthrough at the time, as it linked a very easy-to-obtain measure (resistivity) to a very important petrophysical property of the rock mediums studied in reservoirs (porosity)[3].

2.2. Complex Resistivity Spectra

Archie's findings reinforced the idea that other possible relations between petrophysical properties and other types of properties could be found. In this context, several authors found that the correlation between complex resistivity spectra and petrophysical properties such as porosity and permeability was even much stronger than single resistivity measurements (see [17],[18],[19],[20]).

[2] Nuclear Magnetic Resonance
[3] For an extended study on Archie's relationship see [16]

Obtaining a complex resistivity spectrum consists on measuring the complex impedance of a fluid saturated medium for several different frequencies. With this procedure we can characterize fluids more robustly than by just using a single resistivity measure. That is due to the fact that different fluids may present a very similar value of resistivity at a certain frequency but very different at some other frequency, making them more likely to be distinguishable by using this method. The final measurement is called complex because it is represented by two components: the magnitude and the phase of the impedance. Some authors have not only found a relation between porosity and permeability with the impedance magnitude of the spectra, but also with their phase (see [21]), meaning that using both these values –magnitude and phase– it is likely that the task of characterizing a well may become easier.

An example of the impedance magnitude of one of these spectra obtained using the prototype described in this paper, for free brine –without any kind of porous medium– is shown in Fig. 1.

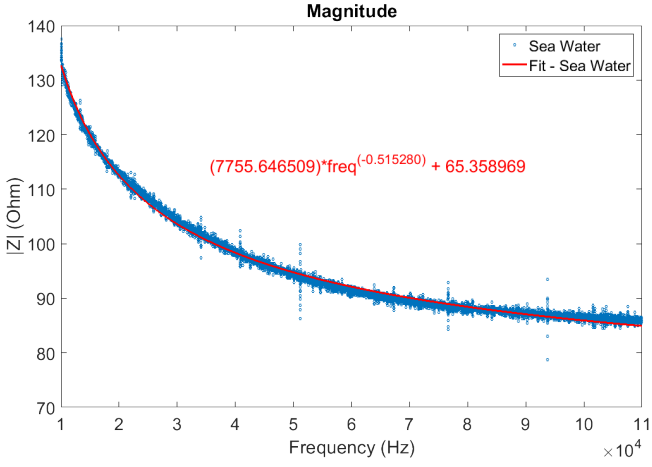

Figure 1: Spectrum of free brine –no porous medium– impedance magnitude over a frequency range from 10 kHz to 110 kHz using the prototype described in this paper. The blue dots represent empirical measurements while the red line an exponential curve fitted to the data.

In this work we use this concept, first to obtain spectra measurements for a well-known porous medium with three different pore sizes in order to link these spectra with the permeability of each type of medium; and secondly to obtain a complex resistivity image of the wall of an artificial well.

3. TESTED FLUIDS AND MEDIUMS

In this work we carried on two main experiments:

1. Extraction of complex spectra for three different porous media (artificial glass sand with different grain sizes).
2. Extraction of a complex resistivity image volume for different fluids.

The main goal of the first experiment is to confirm the relation between permeability and complex resistivity. For

this experience we have used a synthetic sand to act as our porous medium. B. Chencarek et al. have recently worked with this synthetic sand creating artificial rock plugs to estimate petrophysical properties from them (see [22]). Using these artificial plugs, each one of them created with a very precise grain size sand, they proved the existance of a relationship between the relaxation times obtained using NMR and the grain size of each plug. In their work, [22] also calculated the permeability of each one of the porous mediums for each grain size, using the laboratories of PETROBRÁS at CENPES (Rio de Janeiro) that are specially dedicated to the purpose of measuring permeability on rock plugs. In this work we have used the permeability values extracted from their work, adapted to the grain size of the mediums we used.

For this first experiment we have used three different grain sizes to emulate three different mediums. These grain sizes ranges are:

1. **Range 1**: $[54, 106]\,\mu m$
2. **Range 2**: $[212, 250]\,\mu m$
3. **Range 3**: $[350, 500]\,\mu m$

Fig. 2 shows all three types of artificial sand at the same scale. This image was obtained using a *Zeiss Axiolab* Microscope with a *Zeiss Achroplan 10X* objective lens. Images were taking using a *Microsoft Lifecam* at CBPF[4].

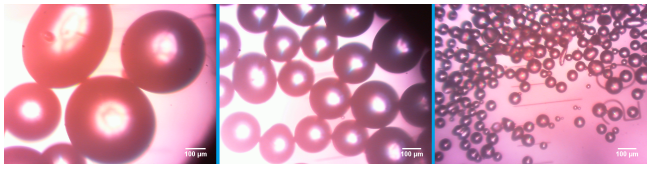

Figure 2: Image of all three different ranges of artificial glass sand used in the first experiment as porous mediums in order to prove the relationship between grainsize and permeability. The scale is the same ($100\mu m$) for all three pictures.

For the second experiment we designed and implemented a system able to obtain complex resistivity images, similarly to borehole electrical imaging systems. For this experiment we have used two fluids with very different resistivities, in order to obtain an image where it would be possible to distinguish between them: paraffin oil and brine.

4. METHODOLOGY

4.1. Complex Resistivity Spectra Measurements System

In order to obtain Complex Resistivity measurements we designed an electronic system using the AD5933 chip (see [23]). This chip is an all-in-one chip specially designed by Analog Devices® to obtain impedance measurements. In order to do so, this chip contains a 27-bit DDS that generates a pure sine wave signal, as well as ADC and DAC converters and a DFT module that make the impedance measure possible. The frequency of the output wave, as well as some other parameters –such as its voltage range, applied gain, frequency step for frequency sweep, etc.– can be controlled easily using the I^2C protocol[5].

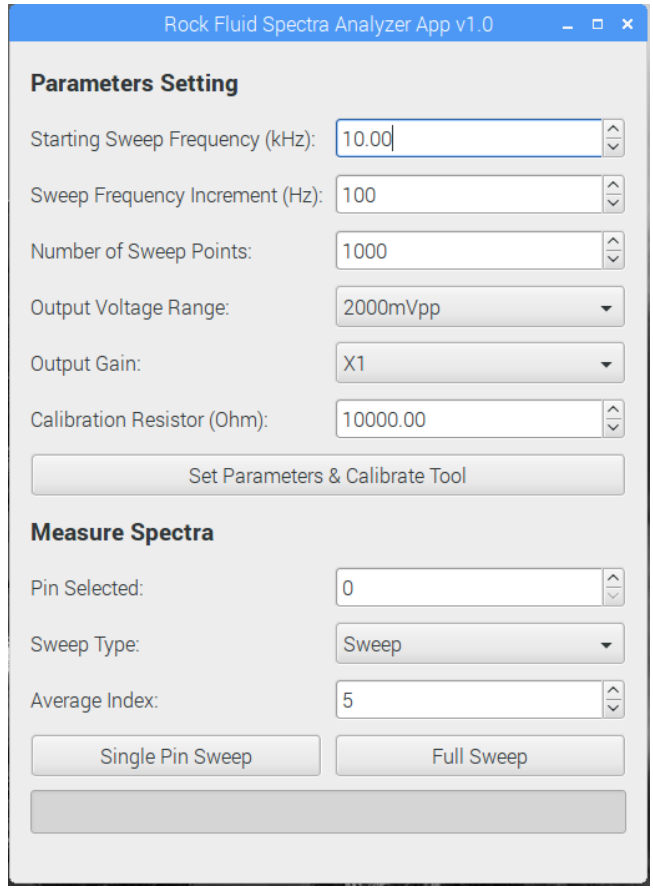

Figure 3: User interface created for this work in order to control and visualize the process of obtaining both single logs of complex resistivity measurements and complex images.

The AD5933 chip has been used over the last years in the implementation of several projects such as measuring bioimpedance for pattern recognition and health control (see [25, 26]). In order to obtain a resistivity spectra from this chip it is necessary to specify the initial frequency of the sweep, the frequency step and the number of points to be swept. All this information, and some other basic configuration, can be set up by the user using an interface we created in C[6]. In order to control all these parameters, as well as the sweeping procedure, we used a Raspberry Pi© board (for more information about this board see [27]). Our C code will run in the Raspberry Pi, communicating with the AD5933 chip using the I^2C communication protocol, and controlling

[4] Centro Brasileiro de Pesquisas Físicas

[5] I^2C is a serial protocol used in electronics for data communication. See [24] for further information.

[6] If interested on the code use to obtain these measurements using the AD5933 board, please contact the corresponding author.

the process of getting and saving all impedance measurements.

The main user interface used in this project is shown in Fig. 3.

4.2. Complex Imaging System

The system we explained in the previous section is able to obtain single spectra logs but not a full image. In order to achieve that we had to create an artificial structure that could recreate a borehole, as well as a system able to take measurements from different positions so that the final result would be a complex image volume. With that purpose we used a PVC[7] pipe to build the sensing cylinder and attached 360 copper pins to it. These pins were uniformly distributed over the surface of the pipe by 20 rows of 9 pins each. Each one of these pairs of pins are used as the probe contacts of our measuring device. In order to be able to measure any kind of fluid and or porous medium we also designed and built an acrylic-glass tank. Henceforth, for imaging purposes the PVC pipe was placed inside the tank, along with the fluids to be imaged. Both this tank and the pipe are shown in Fig. 4, b).

Each pair of pins in the pipe will be represented as a voxel[8] in the final image volume. In order to measure impedance using the AD5933 we must put in its out/in probes the impedance to be measured only. This means that we must connect only one pair of pins with the AD5933 chip at a time. As the AD5933 chip uses an analog wave to measure the impedance it was required to design an analog switch system that would be able to demultiplex this analog signal into each pair of pins. In order to do so we used the analog switch chip CD4066 (for its datasheet, see [28]). The function of this chip is to place the measuring signal coming from the AD5933 into a certain pair of pins in the pipe, according to a certain controlling signal. On the other hand, these analog switches are controlled by the controller system –Raspberry Pi– using an interface of 16-to-1 demultiplexers DM74LS154 chip (see [29]). In order to control which pin is enabled at any time, we use an 8-bit word coming out of the Raspberry Pi. That way, each combination of digits enables a single pair of pins. The whole imaging system can be seen in Fig. 5.

5. RESULTS

The results for each experiment are presented in this section.

[7] PVC: Poly vynil plastic.

[8] As our final image will be a volume of images –one for each frequency–, each pipe pin will produce a voxel, and not a pixel.

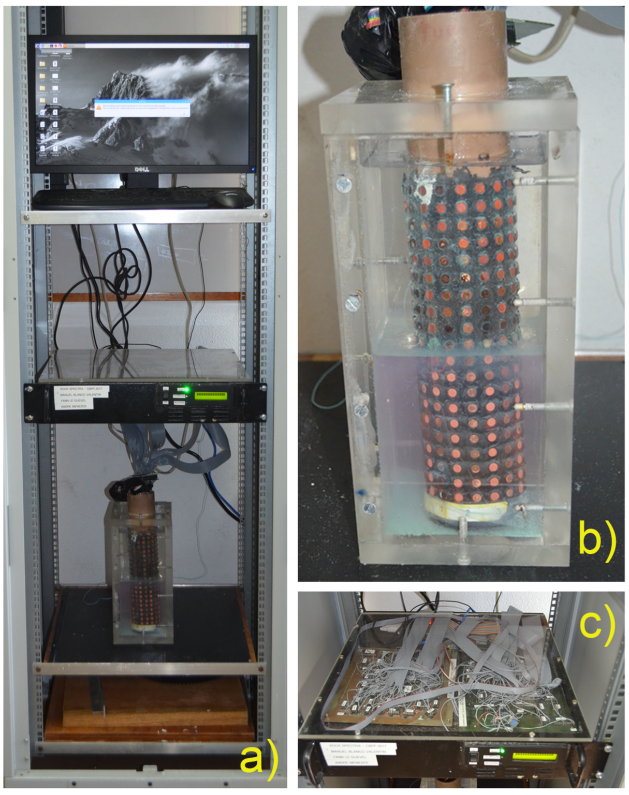

Figure 4: Montage of three images showing the system we built for complex resistivity imaging: a) Whole system with the tank, the pipe and the electronics controller system; b) Close-up of the tank and the pipe, filled with brine –bottom– and paraffin oil –top– as used for the second experiment; c) Close-up of the electronics controller and analog DEMUX system.

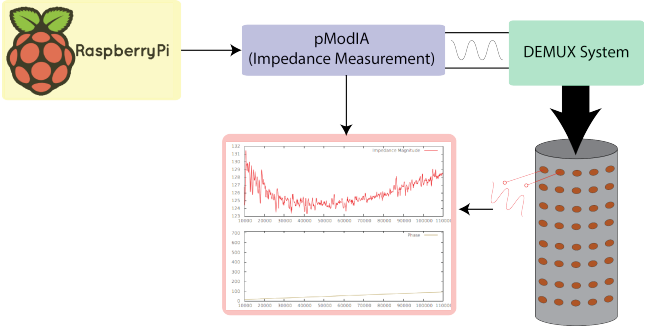

Figure 5: Block Diagram

5.1. Experiment 1 - Spectra measurements and permeability correlation

In this experiment we used fresh brine water to saturate three different porous mediums using the artificial sand described in Section 3. Each one of these mediums had a different grain-size (the first within a range between 54 and 106 μm, the second between 212 and 250 μm and the third one between 350 and 500 μm). For each one of these mediums we carried on several frequency sweep measurements without moving the probes, nor changing the conditions. The frequency sweep we carried on had 1000 frequency points,

Table I: Fitting Parameters obtained for the first test. Each row represents a type of medium tested: Pure Brine, Glass Sand with Range 1 diameter, Glass Sand with Range 2 diameter and Glass Sand with Range 3 diameter. These parameters correspond to the fitting expression presented in (3).

Fit. Param.	SeaWater	Range 1	Range 2	Range 3
a	7755.64	108445.96	384041.03	187090.83
b	-0.51	-0.82	-0.95	-0.88
c	65.36	253.03	233.32	209.74
k_e	–	7000	24500	34000

starting at 1 kHz and going up to 100 kHz. We repeated the experiment 20 times in order to get a reasonable amount of information to extract some statistics about it.

The results obtained for this test are shown in Fig. 6. On that chart, dots represent real measurements while lines are single-term exponential curves fitted for each test. The curved used to fit each curve[9] is presented in (3).

$$f_i(x) = a_i \cdot e^{b_i} + c_i \tag{3}$$

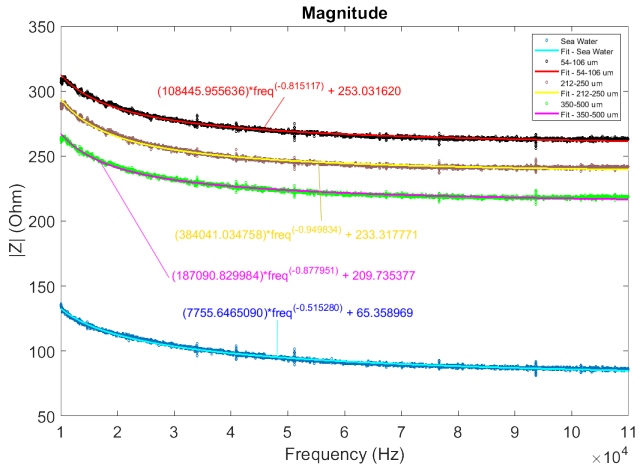

Figure 6: Impedance spectra for the three different grain-sizes brine saturared glass sand used in experiment 1, plus free –with no porous medium– fresh brine/sea-water. As one can see, different grain sizes of the porous medium result in different spectra. All spectra were fitted using the single-term exponential shown in (3).

As introduced in Section 3, [22] calculated the permeability values for each type of these artificial sand mediums. We can, at this point, obtain the correlation between the extracted fitting parameters for each test and their permeability measures that [22] calculated in their work. Both these fitting parameters and respective calculated estimated permeability

[9] Intuitively all spectra seem to be exponential decays. This is the reason why it was proposed to use an exponential curve to fit them. Using a first-order exponential all fits obtained an R^2 coefficient above 99% and, therefore, the possibility of adding terms to the exponential equation used to fit the curves was discarded.

Table II: Correlation coefficient between each one of the fitted parameters *a*,*b* and *c*, using the expression presented in (3) for each tested grain-size with their respective estimated permeability measurements. High values of correlation –positive or negative– indicate strong relation between two variables.

	Fit. Param.		
	a	*b*	*c*
Correlation	43.50%	-60.86%	-97.57%

(k_e) in milidarcies for each type of medium is shown in Table I.

At this point, we can extract Pierson's correlation coefficient between each one of the fitted parameters and the permeability values, to see if there is any kind of relation between them. Table II shows these correlation values.

Even though obtained data may be insufficient for extracting definitive statistical information, we can find an analytic solution that relates permeability with the parameter that has a higher correlation with permeability: parameter c. This analytic equation is shown in (4).

$$\widetilde{k_e} = -11.20 \cdot c_i^2 + 4559.00 \cdot c_i - 4.26 \cdot 10^{+5} \tag{4}$$

5.2. Experiment 2 - Complex resistivity image

In this second experiment we used the methodology and the system described in Section 4 to obtain complex resistivity images from two different and non-miscible fluids: brine and paraffin oil. We used a starting frequency of 10 kHz, a step frequency of 1 kHz and a total of 1000 points for each sweep. The final image is represented by a $20 \times 9 \times 1000$ matrix where each 20×9 slice represents an image that captures the impedance of the system for a certain frequency.

Paraffin oil and brine have very different values of impedance, which makes them a perfect example for testing the imaging system. Brine presents a much higher conductivity than brine and, therefore, should appear in the final image as a darker area. The images of the magnitude –a), b) and c)– and the phase –d), e) and f)– components of the impedance for this test are shown in Fig. 7.

As it can be seen on this image, the contrast between paraffin oil resistivity –mid-top of the images in Fig. 7– and brine resistivity –mid-bottom of the images in Fig. 7– is very clear. Even so, this contrast only changes slightly over the frequency sweep for both phase and magnitude.

6. CONCLUSIONS

In this work we address the relation between complex resistivity spectra for different mediums and their formation permeability. We have also obtained a complex resistivity image over a swept range of frequencies. These tests allow us to conclude:

1. As shown in Fig. 6, different grain-sizes present different resistivity magnitude spectra, meaning that the

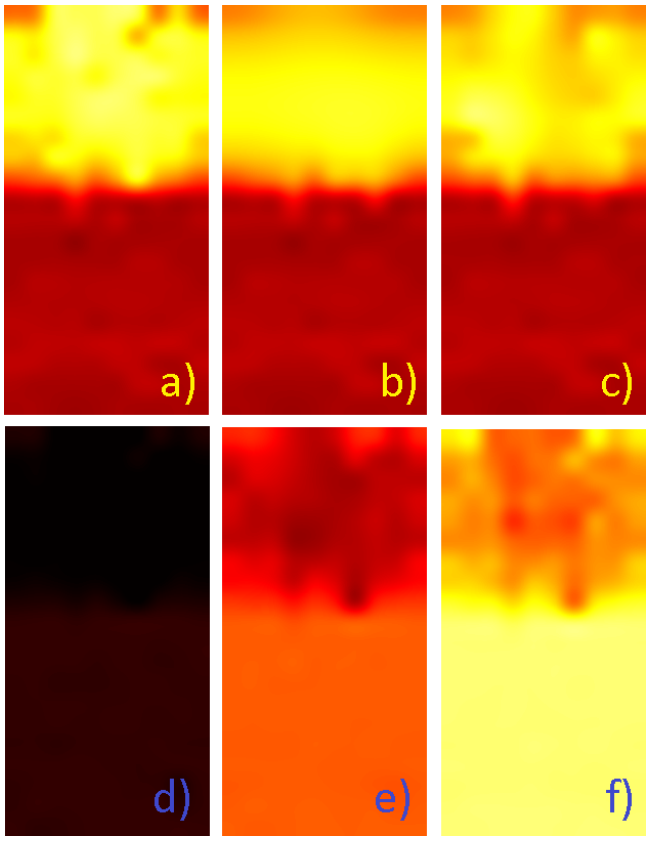

Figure 7: Complex Resistivity Images for test 2 using brine –mid bottom part of the images– and paraffin oil –mid upper part of the images–. All three images in the top –a), b) and c)– represent the magnitude component of the impedance while the ones in the bottom –d), e) and f)– represent the phase component of the impedance over different frequencies. Images a) and d) were obtained at a frequency of 10 kHz; images b) and e) were obtained at a frequency of 51 kHz; and images c) and f) were obtained at a frequency of 94 kHz.

grain-sizes of the porous mediums used in this work might be characterized using them. Even though the curves obtained in this work are extremely similar one to each other, this might not be the case for different types of mediums. In our case we used the same type of pure artificial sand, varying only the grain-size between each test. Despite the fact that the curves were very similar, this might not be the case with other heterogeneous materials. In fact the similarities in the curve might be related to the simplicity of our samples. Therefore, different kinds of more heterogeneous materials and porous mediums may produce more distinguishable spectra.

2. As intuition suggests, the bigger the grain size of the porous medium tested, the closer the spectra is to the one of pure brine water. That is so because the mediums tested in this work were saturated with brine. Big grain sizes will produce big pores between them which will create, virtually, more space between them and will, therefore, allow more electric flow through them; while small grain sizes will produce small pores, creating a more resistive environment for the electrical current to flow through it. This is exactly the behaviour observed in Fig. 6.

3. The fitting parameter c obtained for each curve presented almost 98% correlation with the permeability measurements for each medium. Even though the tests were carried out using only three different grain sizes and a single material –glass sand–, this suggests that there might be a very strong correlation between permeability and this parameter. Looking at (3) we can see that this term, c represents only the offset component of the fitting (value of the exponential curve in the limit, at inifnite frequency). This means that, apparently, the correlation between permeability and the spectra obtained does not depend on the shape of the spectra, but rather on its offset –for the tested material–. In other words, using a single-point measurement of resistivity, at any frequency, we could probably obtain the same type of correlation with permeability. However, as stated before, this might not be true for different types of materials other than the artificial sand tested here. If other materials present different spectra shapes, characterizing them by using a single point measurement of impedance may lead to misclassification and errors and it would be essential, therefore, to extract a full range spectra, as we proposed in this work, to characterize them accurately.

4. The relation between permeability and complex spectra shown in this work could lead to a new application in well-logging tools on which frequency-swept volumes of electrical impedance measurements could help geologists characterize the lithology of the studied field much better, and even obtain estimated permeability images of the well-wall from them.

5. The concept of obtaining a complex resistivity image volume from complex spectra was tested in Section 5.2. The obtained image shows that it is possible to create these kinds of images. Even though there was no significant change of contrast in the images for the swept range of frequencies, it is possible, as we mentioned before, that this contrast changes for different materials. In the authors opinion, the resultant images that could be obtained in a real–field soil test might present distinguishable contrast over different frequencies.

7. FUTURE WORK

We plan to test the proposed methodology in different types of materials such as real rock or sand to check whether the relation with permeability found in this paper is hold and whether this relation can be really described using an exponential curve fit. On the other hand, it would also be interesting to evaluate whether it is feasible or not to obtain an estimated permeability image from a measured spectra volume using the implemented system.

Acknowledgments

This work was made possible by cooperation agreement between CENPES/PETROBRÁS and CBPF. M. B. Valentín would like to thank B. Chencarek for his help during the implementation of the methodology and his insights regardind the results; A. Persechino for his help and availability to obtain the images of the spheres using the optimal microscope; and also A. Menezes for his help during the implementation of the electronics system built for this work.

Bibliography

[1] Philip Kearey, Michael Brooks, and Ian Hill. *An introduction to geophysical exploration*. John Wiley & Sons, 2013.

[2] Rodney Calvert. *Insights and methods for 4D reservoir monitoring and characterization*. Society of Exploration Geophysicists and European Association of Geoscientists and Engineers, 2005.

[3] Darwin V Ellis and Julian M Singer. *Well logging for earth scientists*, volume 692. Springer, 2007.

[4] Gustave E Archie et al. The electrical resistivity log as an aid in determining some reservoir characteristics. *Transactions of the AIME*, 146(01):54–62, 1942.

[5] Stefan M Luthi. Electrical borehole imaging. In *Geological Well Logs*, pages 74–123. Springer, 2001.

[6] Henry Darcy. *Les fontaines publiques de la ville de Dijon: exposition et application...* Victor Dalmont, 1856.

[7] API RP40. Recommended practices for core analysis. *Feb*, 1998.

[8] LJ Klinkenberg et al. The permeability of porous media to liquids and gases. In *Drilling and production practice*. American Petroleum Institute, 1941.

[9] Aytekin Timur et al. An investigation of permeability, porosity, and residual water saturation relationships. In *SPWLA 9th annual logging symposium*. Society of Petrophysicists and Well-Log Analysts, 1968.

[10] A Kohli and P Arora. Application of artificial neural networks for well logs. In *IPTC 2014: International Petroleum Technology Conference*, 2014.

[11] Shahab Mohaghegh, Reza Arefi, Samuel Ameri, D Rose, et al. Design and development of an artificial neural network for estimation of formation permeability. *SPE Computer Applications*, 7(06):151–154, 1995.

[12] Baouche Rafik and Baddari Kamel. Prediction of permeability and porosity from well log data using the nonparametric regression with multivariate analysis and neural network, hassi r mel field, algeria. *Egyptian Journal of Petroleum*, 26(3):763–778, 2017.

[13] Salaheldin Elkatatny, Mohamed Mahmoud, Zeeshan Tariq, and Abdulazeez Abdulraheem. New insights into the prediction of heterogeneous carbonate reservoir permeability from well logs using artificial intelligence network. *Neural Computing and Applications*, pages 1–11, 2017.

[14] Dahai Chang, Harold J Vinegar, Chris Morriss, Chris Straley, et al. Effective porosity, producible fluid and permeability in carbonates from nmr logging. In *SPWLA 35th Annual Logging Symposium*. Society of Petrophysicists and Well-Log Analysts, 1994.

[15] Hugh Daigle and Brandon Dugan. Extending nmr data for permeability estimation in fine-grained sediments. *Marine and Petroleum Geology*, 26(8):1419–1427, 2009.

[16] Peter J Tumidajski, AS Schumacher, S Perron, P Gu, and JJ Beaudoin. On the relationship between porosity and electrical resistivity in cementitious systems. *Cement and concrete research*, 26(4):539–544, 1996.

[17] Jan Henrik Norbisrath. *Complex resistivity spectra in relation to multiscale pore geometry in carbonates and mixed-siliciclastic rocks*. PhD thesis, University of Miami, 2016.

[18] Maosong Tong and Honggen Tao. Permeability estimating from complex resistivity measurement of shaly sand reservoir. *Geophysical Journal International*, 173(2):733–739, 2008.

[19] Jan Henrik Norbisrath. *Complex resistivity spectra in relation to multiscale pore geometry in carbonates and mixed-siliciclastic rocks*. PhD thesis, University of Miami, 2016.

[20] David Huntley. Relations between permeability and electrical resistivity in granular aquifers. *Groundwater*, 24(4):466–474, 1986.

[21] Leonardo Pereira Marinho and Carlos Alberto Dias. Complex resistivity measurements on plugs from corvina oil field, campos basin, brazil. In *15th International Congress of the Brazilian Geophysical Society & EXPOGEF, Rio de Janeiro, Brazil, 31 July-3 August 2017*, pages 929–937. Brazilian Geophysical Society, 2017.

[22] Bruno Chencarek, Maury Duarte Correia, Moacyr do Nascimento, Alexandre M. Souza, and Ivan S. Oliveira. Processo para produção e caracterização de rochas sintéticas com porosidade controlada para aplicações em petrofísica por rmn de alto e baixo campo. *Notas Técnicas do CBPF*, 2017.

[23] Analog Devices. Ad5933 datasheet, 2007.

[24] Philips Semiconductors. The i2c-bus specification. *Philips Semiconductors*, 9397(750):00954, 2000.

[25] Javier Ferreira, Fernando Seoane, Antonio Ansede, and Ramon Bragos. Ad5933-based spectrometer for electrical bioimpedance applications. In *Journal of Physics: Conference Series*, volume 224, page 012011. IOP Publishing, 2010.

[26] C Margo, J Katrib, Mustapha Nadi, and Amar Rouane. A four-electrode low frequency impedance spectroscopy measurement system using the ad5933 measurement chip. *Physiological measurement*, 34(4):391, 2013.

[27] Eben Upton and Gareth Halfacree. *Raspberry Pi user guide*. John Wiley & Sons, 2014.

[28] Texas Instruments. Cd4066b cmos quad bilateral switch, 2015.

[29] Fairchild Semiconductor. Dm74ls154 4-line to 16-line decoder/demultiplexer. *Retrieved April*, 20:2004, 2000.

Notas Técnicas é uma publicação de trabalhos técnicos relevantes, das diferentes áreas da física e afins, e áreas interdisciplinares tais como: Química, Computação, Matemática Aplicada, Biblioteconomia, Eletrônica e Mecânica entre outras.

Cópias desta publicação podem ser obtidas diretamente na página web http://revistas.cbpf.br/index.php/nt ou por correspondência ao:

Centro Brasileiro de Pesquisas Físicas
Área de Publicações
Rua Dr. Xavier Sigaud, 150 – 4º andar
22290-180 – Rio de Janeiro, RJ
Brasil
E-mail: alinecd@cbpf.br/valeria@cbpf.br
http://portal.cbpf.br/publicacoes-do-cbpf

Notas Técnicas is a publication of relevant technical papers, from different areas of physics and related fields, and interdisciplinary areas such as Chemistry, Computer Science, Applied Mathematics, Library Science, Electronics and Mechanical Engineering among others.

Copies of these reports can be downloaded directly from the website http://notastecnicas.cbpf.br or requested by regular mail to:

Centro Brasileiro de Pesquisas Físicas
Área de Publicações
Rua Dr. Xavier Sigaud, 150 – 4º andar
22290-180 – Rio de Janeiro, RJ
Brazil
E-mail: alinecd@cbpf.br/valeria@cbpf.br
http://portal.cbpf.br/publicacoes-do-cbpf